Surface evolution of amorphous nanocolumns of Fe–Ni grown by oblique angle deposition

Senoy Thomas,[1] S. H. Al-Harthi,[2] R. V. Ramanujan,[3] Zhao Bangchuan,[4] Liu Yan,[3] Wang Lan,[4] and M. R. Anantharaman[1,a)]

[1]*Department of Physics, Cochin University of Science and Technology, Cochin 682022, India*
[2]*Department of Physics, College of Science, Sultan Qaboos University, PO Box 36, Postal Code 123, Muscat, Sultanate of Oman*
[3]*School of Materials Science and Engineering, Nanyang Technological University, Singapore 639798, Singapore*
[4]*School of Physical and Mathematical Sciences, Nanyang Technological University, Signapore 637371, Singapore*

The growth of Fe–Ni based amorphous nanocolumns has been studied using atomic force microscopy. The root mean square roughness of the film surface increased with the deposition time but showed a little change at higher deposition time. It was found that the separation between the nanostructures increased sharply during the initial stages of growth and the change was less pronounced at higher deposition time. During the initial stages of the column growth, a roughening process due to self shadowing is dominant and, as the deposition time increases, a smoothening mechanism takes place due to the surface diffusion of adatoms. © *2009 American Institute of Physics*. [DOI: 10.1063/1.3080615]

Soft magnetic alloys of Fe–Ni are of great interest due to their proven applications in power conversion, conditioning and generation, transformer cores, electromagnetic shielding, and sensors.[1–3] The amorphous structure of these alloys plays a major role in the reduction of magnetic anisotropy energy and the corresponding modification of properties such as coercivity and permeability. In addition, the random atomic structure leads to increase in resistivity making them suitable for high frequency applications. With the advent of amorphous materials exhibiting excellent soft magnetic properties, the thin film form of this material are also important from an application point of view. The development of nanostructured soft magnetic materials makes it possible to miniaturize magnetic devices and integrate them, e.g., in microelectromechanical systems and sensor applications

Small magnetic structures, in principle, can be patterned by e-beam lithography. However, this technique requires expensive instrumentation and is not very versatile. For instance, the e-beam technique can introduce phase transformations in materials upon exposure.[4] An alternative to this is thin film deposition at oblique angles.[5] This technique utilizes physical vapor deposition to deposit films on a substrate oriented at an oblique angle to the vapor source. The vapor atoms travel to a fixed substrate at large oblique angle respective to the surface normal of the substrate. The evaporant nucleates on the substrate and the region behind the nucleus does not receive any further vapor because of the shadowing by the nucleus. Therefore, vapor will only be deposited onto the nucleus. This preferential growth dynamics gives rise to the formation of columnar structures. The morphology of such films will be a resultant of the competition between smoothening due to surface diffusion of adatoms and roughening due to the self shadowing process. The film surfaces grown under these two competing process usually generate fascinating self affine patterns.[6–8]

For the synthesis of thin films with both a well-defined value of the surface roughness and well-defined surface morphologies, an understanding on the interplay between the mechanisms involved in the growth process of thin films is essential. From a fundamental point of view, this will enable a classification of the underlying physical phenomena controlling a given growth process. From an applied point of view, a detailed knowledge of the scaling behavior of the rough surface will aid in synthesizing surfaces with well defined roughness and geometry. While so much work has been devoted to understand the effect of deposition parameters on the morphology of elementary metal nanocolumns,[9–11] there has been less efforts to understand the growth mechanisms of nanostructures of amorphous alloys.

In this study, the authors demonstrate the preparation of Fe–Ni based amorphous nanocolumns by oblique angle deposition employing thermal evaporation technique. The focus is on Fe–Ni based amorphous alloys due to their interesting soft magnetic properties as well as their wide application potential in the field of sensors.[12] Atomic microscopy is employed to quantitatively investigate the mechanisms involved in the growth process of obliquely deposited magnetic nanostructures.

Commercially available Metglas 2826 MB ribbon of composition $Fe_{40}Ni_{38}Mo_4B_{18}$ was employed as a source material to deposit Fe–Ni thin films on silicon substrates. Silicon substrates were cleaned with acetone, ethanol, and trichloroethylene and were immediately loaded into the vacuum chamber. The films were deposited by thermal evaporation using a current of 25 A at a base pressure of 1×10^{-5} mbar onto substrates oriented at an oblique angle of 40° to the flux. The base pressure of $\sim 1 \times 10^{-5}$ mbar was achieved by a diffusion pump backed with a rotary pump. The source to substrate distance was $\sim$26 cm. A set of samples were deposited at an oblique angle of 40° with the

---

a)Author to whom correspondence should be addressed. Electronic mail: mraiyer@gmail.com.
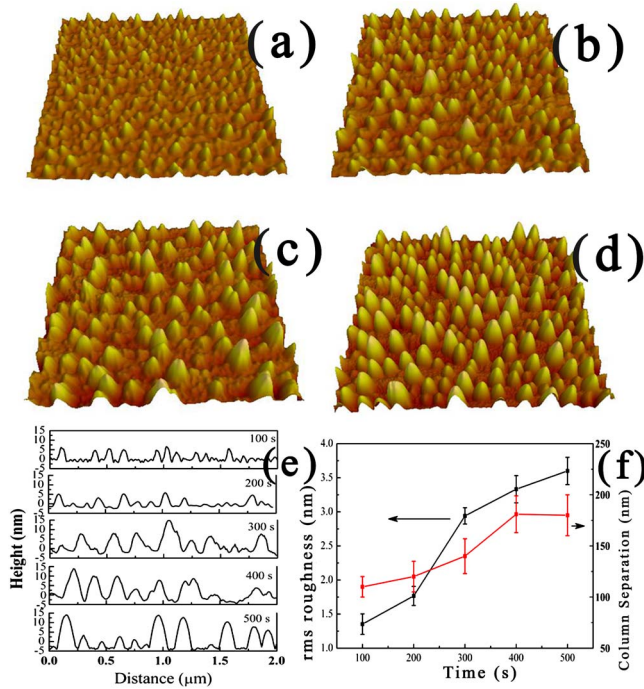
FIG. 1. (Color online) (a) AFM image for a film obtained after a deposition time of 200 s, (b) 300 s, (c) 400 s, and (d) 500 s. An AFM line profile on different samples is shown in (e) and (f) plot of rms roughness vs deposition time and distance between columns vs deposition time. All AFM images are 2×2 μm^2, with z scale 20 nm.

same source to substrate distance ($\sim$26 cm) but with different deposition time (100, 200, 300, 400, and 500 s). The average deposition rate measured by a step profilometer was 6 nm/min. X-ray photoelectron spectroscopy, x-ray diffraction, and transmission electron microscopy were employed to characterize the films, and it was found that the films prepared under different deposition conditions consisted of an amorphous phase with a composition of $Fe_{55}Ni_{45}$.

Images of the film surface were acquired using a Digital Instruments Nanoscope atomic force microscope (AFM) operated in the tapping mode using an etched single crystal silicon tip. 2×2 μm^2 areas were scanned with a resolution of 256×256 pixels. AFM data was used to evaluate the rms roughness. In addition, the surface microstructure was studied using power spectral density (PSD) function calculations. The two-dimensional PSD (2D PSD) calculations were performed using the software provided by Digital Instruments.

Figures 1(a)–1(d) show the AFM images of Fe–Ni film surfaces, which were grown at different conditions as described above. The comparison between column height and total thickness of the film suggests that filling of voids in between the column is taking place during the growth and resulting in a layer plus island type geometry. It can be seen that the lateral size as well as surface height (peak to valley) of the columns grows with increase in the deposition time.

Figure 1(f) depicts plot of rms roughness versus deposition time. The change of roughness up to a deposition time of 300 s is sharp while it is gradual for higher value of deposition time. During the initial stages of growth, the microstructure is strongly affected by shadowing. At this time, the grains grow in a uncorrelated fashion from the nuclei formed initially. Such an independent growth should agree with the sharp change in roughness for short deposition time. At higher deposition times, the change in roughness is minimal,
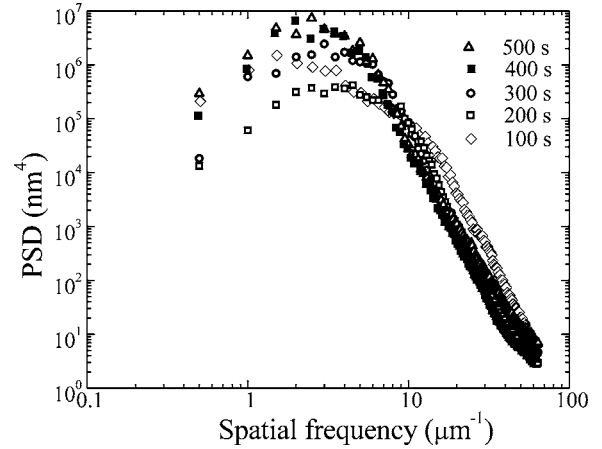

FIG. 2. PSD function curves calculated for thin films obtained with different deposition time.

implying that a smoothening mechanism by surface diffusion is also prominent. Also, as the deposition time increases, the lateral growth of columns occurs, and this can be due to the surface diffusion of adatoms. The lateral growth of the columns at higher deposition time can be evidenced from the AFM line scans depicted in Fig. 1(e). Thus for higher deposition time surface diffusion also plays an important role in the growth process of films.

2D PSD calculations were performed for the different films prepared. The 2D PSD spectrum provides the variation of PSD magnitude as a function of spatial frequencies. The PSD analysis allows quantification of the surface structure. Figure 2 shows log-log plots of power spectra PSD (f) calculated for thin films obtained at different deposition time.

The log-log plot of 2D PSD can be divided into two distinct regimes. The low frequency part which gives an indication of the periodicity of nanostructures and a high frequency part where the PSD distribution is decaying with frequency following a power law $\sim f^{-\gamma}$, where f is the frequency and γ is the power.

By fitting PSD(f) $\alpha f^{-\gamma}$ to the correlated part, we obtain $\gamma \sim -5.28, -5.4, -5.61, -6.33$, and -6.69 for the films grown at deposition time 500, 400, 300, 200, and 100 s respectively. Since γ is related to the roughness exponent α by the equation[13] $\alpha = (\gamma - d)/2$, where the line scan dimension d is 2 in our case, the roughness exponent has a value $\alpha = 1.64, 1.7, 1.8, 2.15$, and 2.34 for the deposition time 500, 400, 300, 200, and 100 s, respectively. It is to be noted that surface diffusion effects that lead to smoothening will lower the exponent. On the other hand, shadowing will increase the exponents.[13] The lowering of roughness exponent at higher deposition time indicates that at higher deposition time, a smoothening mechanism by surface diffusion is also prominent in the growth process of the film. This supports our inferences derived from the roughness versus deposition time plots [Fig. 1(f)].

Moreover a nonsaturation behavior of PSD function curves can be observed in the low frequency regime. The nonsaturation behavior of PSD has been previously observed in mound structures grown by oblique angle deposition technique.[14] Figure 1(f) shows column separation versus deposition time. It is clear that the column separation increases with deposition time and shows saturation at higher deposition time. The column separation is exactly the shad-
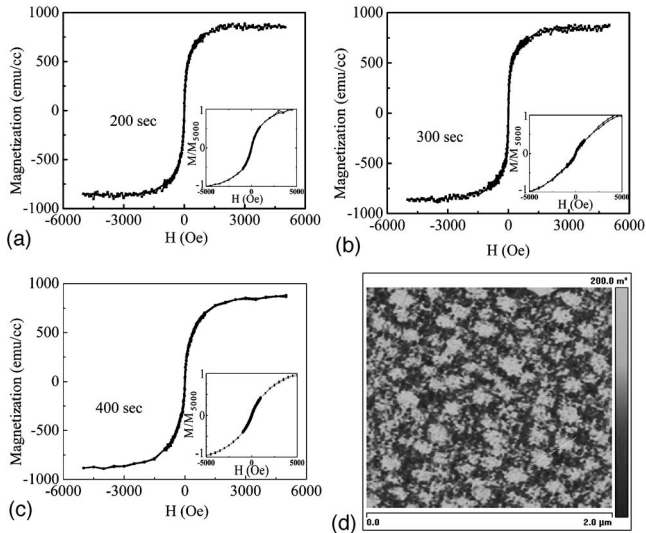
FIG. 3. Room temperature hysteresis loops for films obtained after a deposition time of 200 s, (b) 300 s, and (c) 400 s in parallel field. Inset shows the corresponding hysteresis loops for perpendicular field and (d) MFM image for a film deposited at 300 s (2×2 μm^2, z scale 200 m Deg).

owing distance. The shadowing length increases with the height of the column according to the equation, $L = h \tan \theta$, where L is the shadowing length, h is the height of the surface feature, and θ is the oblique angle. Initially, due to the random effect during growth, some surface features become more prominent than nearby ones, and they get additional flux resulting in an increase in the shadowing length. As the deposition time increases, the columns become more uniform in length, and after a critical deposition time shadowing length does not increase significantly.

The room temperature hysteresis curve for films deposited at 200, 300, and 400 s recorded both in the in plane and out of plane geometry are depicted in Figs. 3(a)–3(c), respectively. The saturation magnetization was found to be ~870 emu/cc. It is to be noted that a low field of ~2000 Oe was only necessary to saturate the magnetization in the in plane while a field as high as 5000 Oe or above could not saturate the material in the out of plane geometry. The vibrating sample magnetometry (VSM) results show that the easy axis of magnetization is in the plane of the film. The magnetic force microscopy (MFM) images are depicted in Fig. 3(d), and this shows the existence of circular domains with an out of plane magnetic component. A comparison of AFM and MFM images shows that there is a one to one correspondence between the domains observed and the islands formed. It is to be noted that imaging was done using a Si tip coated with a CoCr thin film (80 nm thick) that was magnetized vertically and at a tip to sample separation (lift height) of 40 nm. The lift height of 40 nm is greater than the film roughness (~3 nm), and so the chances of topographical influence on the MFM signal can be negligible. In systems where shape anisotropy is predominant, the easy axis of magnetization will be along the direction of long axis. If there are deposits in between the columns, the portion close to the substrate will become a continuous layer and the geometry of the whole system will be a layer plus island type

in which islands are arranged on top of the layer. Due to the absence of magnetocrystalline anisotropy, the magnetization direction will be more influenced by the shape anisotropy. In the layer, where the long axis is along the plane of the substrate, the magnetic direction will be in plane. While in the islands, where the long axis is perpendicular to the plane of the substrate, the magnetic direction will be out of plane. The magnetization measurements using VSM is rather a bulk technique and one will only notice signatures of in plane anisotropy because of the domination of the contributions emanating from the layer. However MFM being sensitive to the local detects the out of plane component from the islands. The measurements show that the perpendicular anisotropy from the columns is small, and this can be due to their small aspect ratio.

In conclusion Fe–Ni based amorphous nanocolumns were grown on Si substrates by oblique angle deposition. The films were grown at different deposition times at an oblique angle of 40°. AFM was employed to quantitatively investigate the surface roughening process in the oblique angle vapor deposited amorphous thin films.

Surface scaling analysis through roughness and PSD spectra showed that at low deposition time, the growth mechanism is dominated by self shadowing, while for higher deposition time surface diffusion is also contributing to the growth process. This situation resulted in the lateral growth of nanostructures at higher deposition times. From an applied point of view, the method of obtaining magnetic nanostructures using this low-technology method is interesting and one should evolve preventive measures against surface diffusion while making attempts to get isolated nanostructures. This can be realized by performing the deposition on a patterned substrate or through substrate rotation.

[1] R. Hasegawa, Mater. Sci. Eng., A **375**, 90 (2004).
[2] M. E. McHenry, M. A. Willard, and E. David, Prog. Mater. Sci. **44**, 291 (1999).
[3] S. X. Wang, N. X. Sun, M. Yamaguchi, and S. Yabukami, Nature (London) **407**, 150 (2000).
[4] M. Sorescu, E. T. Knobbe, and D. Barb, Phys. Rev. B **51**, 840 (1995).
[5] M. M. Hawkeye and M. J. Brett, J. Vac. Sci. Technol. A **25**, 1317 (2007).
[6] A. Yanguas-Gil, J. Cotrino, A. Walkiewicz-Pietrzykowska, and A. R. González-Elipe, Phys. Rev. B **76**, 075314 (2007).
[7] A. Borrás, A. Yanguas-Gil, A. Barranco, J. Cotrino, and A. R. González-Elipe, Phys. Rev. B **76**, 235303 (2007).
[8] M. A. Auger, L. Vázquez, O. Sánchez, M. Jergel, and R. Cuerno, J. Appl. Phys. **97**, 123528 (2005).
[9] K. Rechendorff, M. B. Hovgaard, J. Chevallier, M. Foss, and F. Besenbacher Appl, Phys. Lett. **87**, 073105 (2005).
[10] M. B. Dolatshahi-Pirouz, M. B. Hovgaard, K. Rechendorff, J. Chevallier, M. Foss, and F. Besenbacher, Phys. Rev. B **77**, 115427 (2008).
[11] H. Alouach and G. J. Mankey, Appl. Phys. Lett. **86**, 123114 (2005).
[12] A. Hernando, M. Vazquez, and J. M. Barandiaran, J. Phys. E **21**, 1129 (1988).
[13] J. Xu, L. Yu, and I. Kojima, J. Appl. Phys. **94**, 6827 (2003).
[14] T. Karabacak, G.-C. Wang, and T.-M. Lu, J. Appl. Phys. **94**, 7723 (2003).